Immunity
Article

Transcriptional Regulation of Germinal Center B and Plasma Cell Fates by Dynamical Control of IRF4

Kyoko Ochiai,[1,7,8] Mark Maienschein-Cline,[2,8] Giorgia Simonetti,[4] Jianjun Chen,[3] Rebecca Rosenthal,[3] Robert Brink,[5] Anita S. Chong,[3] Ulf Klein,[4] Aaron R. Dinner,[2,9] Harinder Singh,[1,6,9,*] and Roger Sciammas[3,9,*]
[1]Departments of Molecular Genetics and Cell Biology
[2]Department of Chemistry
[3]Department of Surgery
The University of Chicago, Chicago, IL 60637, USA
[4]Herbert Irving Comprehensive Cancer Center, Departments of Pathology & Cell Biology and Microbiology & Immunology, Columbia University, New York, NY 10032
[5]Immunology Research Program, Garvan Institute of Medical Research, Darlinghurst, NSW 2010, Australia
[6]Discovery Immunology, Genentech, San Francisco, CA 94080, USA
[7]Present address: Department of Biochemistry, Tohoku University Graduate School of Medicine, Seiryo-machi 2-1, Sendai, Japan
[8]These authors are co-first authors
[9]These authors are co-senior authors
*Correspondence: singh.harinder@gene.com (H.S.), rsciamma@uchicago.edu (R.S.)
http://dx.doi.org/10.1016/j.immuni.2013.04.009

SUMMARY

The transcription factor IRF4 regulates immunoglobulin class switch recombination and plasma cell differentiation. Its differing concentrations appear to regulate mutually antagonistic programs of B and plasma cell gene expression. We show IRF4 to be also required for generation of germinal center (GC) B cells. Its transient expression in vivo induced the expression of key GC genes including *Bcl6* and *Aicda*. In contrast, sustained and higher concentrations of IRF4 promoted the generation of plasma cells while antagonizing the GC fate. IRF4 cobound with the transcription factors PU.1 or BATF to Ets or AP-1 composite motifs, associated with genes involved in B cell activation and the GC response. At higher concentrations, IRF4 binding shifted to interferon sequence response motifs; these enriched for genes involved in plasma cell differentiation. Our results support a model of "kinetic control" in which signaling-induced dynamics of IRF4 in activated B cells control their cell-fate outcomes.

INTRODUCTION

Germinal Center (GC) B cells and plasma cells (PC) develop following the activation of naive B cells with cognate antigen in combination with signals from T helper cells and dendritic cells (Goodnow et al., 2010). These distinct cellular states, GC and PC, perform key roles in humoral immunity against microbes by enabling generation of high-affinity antibodies and their robust expression and secretion, respectively. Considerable progress has been achieved in the analysis of transcription factors that are required for the generation of GC B cells and their plasma cell counterparts; however, the molecular mechanisms by which such regulators orchestrate these alternative cellular states and the transition from the GC to the PC differentiation programs are incompletely understood.

The identity and function of plasma cells is dependent on the transcription factors Blimp1, Xbp1, and IRF4 (Nutt et al., 2011). In contrast, GC B cell development requires the transcription factors Bcl6, Pax5, Bach2, and Obf1 (Nutt et al., 2011). Blimp1 and Bcl6 function to counter regulate each other's expression. This reciprocal negative feedback is considered to play a major role in stabilizing the alternate programs of gene expression.

We have proposed that the transcription factor IRF4 is a pivotal regulator of B cell-fate dynamics upon antigen encounter (Sciammas et al., 2006, 2011). This is based on our findings that IRF4 is required for class switch recombination (CSR) and plasma cell differentiation. It does so by upregulating AID and Blimp1 expression, respectively. We have demonstrated, by using a variety of approaches, that differing IRF4 concentrations underlie the generation of these alternative cell states. These experimental analyses have led to the formulation of a "kinetic control" model for the regulation of B cell-fate dynamics spanning the CSR and plasma-cell states (Sciammas et al., 2011; see also Muto et al., 2010). According to this model, the rate of accumulation of IRF4 induced by the BCR determines the duration for which such a cell expresses AID and therefore can undergo CSR and also somatic hypermutation (SHM). Increased expression of IRF4 beyond a critical threshold results in IRF4 activation of the *Prdm1* (encoding Blimp1) locus and terminal differentiation into a plasma cell. This is accompanied by repression of *Aicda* (encoding AID) expression and CSR, as well as SHM. However, it remains to be determined whether this regulatory model is applicable to T-dependent B cell responses in vivo. It has been suggested that IRF4 is dispensable for the GC response in vivo (Klein et al., 2006). However, this conclusion was based on the use of a conditional allele of IRF4 whose deletion is initiated after antigen encounter, raising the possibility that IRF4 protein was not sufficiently depleted in precursors of GC B cells in these mice. Therefore, we sought to address the role of

IRF4 in regulating generation of GC B cells by using alternative genetic strategies.

IRF4 is a member of the IRF superfamily of transcription factors most highly related to IRF8 (Eisenbeis et al., 1995). Although IRF8 is expressed in activated and GC B cells, it has been shown to be dispensable for antigen-dependent B cell responses (Feng et al., 2011). IRF4 and IRF8 bind with much lower affinity to the GAAA motif contained within the canonical interferon sequence response element (ISRE). Instead they are recruited to high affinity Ets-IRF composite motifs (EICE) through their interaction with the transcription factors PU.1 or SpiB (Brass et al., 1999; Eisenbeis et al., 1995). The latter are related Ets family members that play key roles in B cell activation and GC B cell function (Garrett-Sinha et al., 2001; Su et al., 1997). Recently IRF4 and IRF8 have shown to cooperatively assemble with BATF containing AP-1 complexes on composite AP-1-IRF (AICE) motifs (Glasmacher et al., 2012). Intriguingly, IRF4 appears to activate the *Prdm1* (Blimp1) locus by binding to a site within a conserved intronic sequence that does not contain an EICE motif nor is associated with PU.1 cobinding (Sciammas et al., 2006). These results raised the possibility that alternate modes of IRF4 genome targeting i.e., PU.1 or SpiB dependent and Ets factor independent may be important in regulating distinct states of gene expression, GC versus PC, within activated B cells.

Herein, by using distinct genetic strategies we demonstrate that IRF4 regulates the generation of GC B cells. It does so by controlling the expression of the *Bcl6* and *Obf1* genes. Furthermore, whereas transient induction of IRF4 in vivo was sufficient to induce GC B cells, sustained and higher concentrations of IRF4 promoted the generation of plasma cells while antagonizing the GC fate. To delineate IRF4 target genes and its modes of genomic interaction that are reflective of the GC or plasma cell programs, we performed chromatin immunoprecipitation sequencing (ChIP-seq) analysis by using an antigen-specific B cell culture system. Kinetic analysis of IRF4 binding to genomic sites, with or without its DNA partner PU.1, was correlated with changes in gene expression. Interestingly, IRF4 cotargeting with PU.1 at EICE motifs was associated with genes involved with B cell activation and the GC response. During these early stages of B cell activation, IRF4 targeting was also associated with AICE motifs. In striking contrast at a later stage, reflective of plasma cells, IRF4 targeting shifted to lower affinity ISRE motifs that enriched for genes involved in plasma cell differentiation. These results provide molecular insight into the concentration-dependent modes of IRF4 action in regulating the GC and PC programs of gene expression. Furthermore, they provide in vivo support for our model of "kinetic control," which posits that the dynamics of accumulation of IRF4 in activated B cells regulate cell-fate outcomes during a humoral immune response.

RESULTS

IRF4 Regulates GC B Cell Differentiation

To analyze requirement of IRF4 in GC B cell responses, we generated mixed bone marrow chimeras with $Irf4^{+/+}$ and $Irf4^{-/-}$ progenitors (see Figure S1A available online). Following hematopoietic reconstitution, the animals were immunized with sheep red blood cells (SRBC) to elicit a T-dependent GC B cell response. Whereas the wild-type (WT) ($CD45.1^+CD45.2^+$) $B220^+$ compartment contained $CD95^+GL7^+$ GC B cells, the $Irf4^{-/-}$ ($CD45.2^+$) $B220^+$ compartment lacked such cells (Figure 1A). Accordingly, Bcl6 expressing cells were not generated within the $Irf4^{-/-}$ population (Figure 1B). The defect in GC B cell formation must be intrinsic to $Irf4^{-/-}$ B cells because the hematopoietic compartment in these chimeric animals contains WT T and dendritic cells. It has been suggested that B cells from $Irf4^{-/-}$ mice are developmentally immature based on expression of CD23 and immunoglobulin M (IgM) (Mittrücker et al., 1997). To exclude the possibility that the severe block in GC B cell differentiation was simply due to a developmental arrest at an immature stage, we analyzed $Irf4^{-/-}$ B cells for expression of CD93, a marker of immature and transitional B cells (Allman et al., 2001). CD93 expression on splenic B cells from $Irf4^{+/-}$ and $Irf4^{-/-}$ mice was indistinguishable (Figure S1B). Moreover, this analysis revealed the basis for the skewed distributions of CD23 and IgM expression in $Irf4^{-/-}$ mice to be likely due to an increase in the proportions of marginal zone B cells (Figures S1C and S1D). Thus the defect in GC B cell differentiation caused by loss of IRF4 is not due to a developmental arrest at an immature B cell stage.

Previously, we suggested that IRF4 was dispensable for GC B cell differentiation based on analysis of $Irf4^{fl/fl}$ mice using a $C\gamma1$-Cre driver that deletes after antigen stimulation of B cells (Klein et al., 2006). The analysis did not rule out the possibility that in this mouse model, the timing of *Irf4* deletion and/or stability of the residual IRF4 protein may have obscured its role in GC B cell differentiation. To test this possibility, we crossed $Irf4^{fl/fl}$ mice with CD19-Cre mice so that deletion of the *Irf4* gene occurred prior to antigen encounter. Importantly, earlier deletion of *Irf4* in B cells resulted in an impaired GC response (Figures 1C and 1D). The conditional *Irf4* allele activates GFP expression concomitant with CRE-mediated deletion (Klein et al., 2006). Staining of splenic tissue sections revealed that the few GCs developing in $Irf4^{fl/fl}$ × CD19-Cre mice were GFP-negative, in contrast with their controls, demonstrating that these residual GCs were formed with B cells in which the *Irf4* allele had not been deleted (Figure 1D). Thus, IRF4 plays an essential and cell-autonomous role in instructing GC B cell differentiation.

IRF4 Regulates *Bcl6* and *Pou2af1* during a GC B Cell Response

To determine whether IRF4 regulates Bcl6 and Obf1 expression within antigen-responding B cells in vivo, we bred the $Irf4^{-/-}$ mouse to the SW_{HEL} mouse in which the B cells are specific for the Hen Egg Lysozyme (HEL) antigen (Phan et al., 2005). SW_{HEL} B cells from WT and $Irf4^{-/-}$ mice were adoptively transferred into CD45.1 mice, which were then immunized with the intermediate affinity HEL^{2X} coupled to SRBC (Figure S2A). Analysis of IRF4 and Bcl6 expression in WT SW_{HEL} responder cells, 4.5 days later, revealed two subsets: $IRF4^{lo}Bcl6^+$ and $IRF4^{hi}Bcl6^-$ (Figure 2A; Figure S2B). Because IRF4 is highly expressed in plasma cells, we confirmed that $IRF4^{hi}Bcl6^-$ population represented plasma cells by their expression of cytoplasmic anti-HEL Ig and reduced B220 (Figure S2C). In contrast, the $IRF4^{lo}Bcl6^+$ population represented GC B cells based on high expression of Bcl6 and B220. Importantly, $Irf4^{-/-}$ SW_{HEL} cells did not generate either Bcl6 expressing cells or plasmablasts. Notably, $Irf4^{-/-}$ SW_{HEL} B cells responded appropriately to

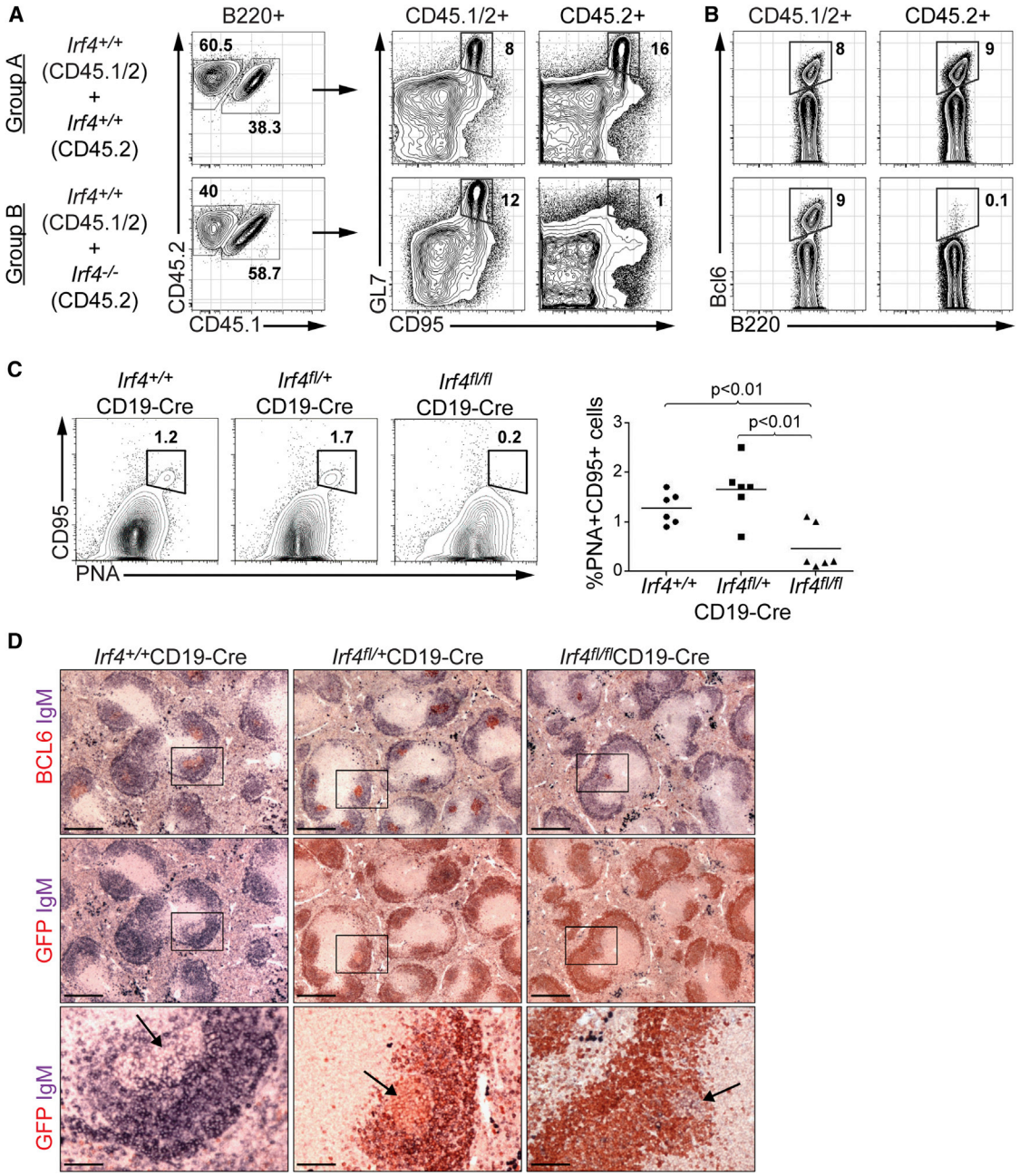

Figure 1. IRF4 Regulates GC B Cell Differentiation

(A and B) We generated 1:1 mixed bone marrow chimeras such that the CD45.1-expressing compartments in groups A and B were reconstituted with *Irf4*$^{+/+}$ hematopoietic progenitors, whereas the CD45.2 expressing compartments were reconstituted with *Irf4*$^{+/+}$ and *Irf4*$^{-/-}$ hematopoietic progenitors, respectively. Reconstituted mice were immunized with SRBC, and GC B cells were analyzed on Day 7 based on expression of GL7 and CD95 or intracellular Bcl6 expression after gating on CD45 polymorphic alleles and the B cell lineage marker B220 as indicated. Data are representative of two independent experiments using five mice per group.

(C) Conditional deletion of *Irf4* in B cells using CD19-Cre. Indicated mice were immunized with SRBC and splenic GC B cells were analyzed on day 14 based on expression of PNA and CD95 after gating on B220. Each point in the right panel represents the numbers of GC B cells from individual mice.

(D) Immunohistochemical analysis of GCs in mice described in (C). Splenic sections were stained for Bcl6, IgM, and GFP as indicated. See also Figure S1.

antigen and engaged T cell help as they underwent multiple cell divisions, albeit with reduced efficiency (Figure S2D) (Phan et al., 2005). Thus, IRF4 plays an essential role in the generation of Bcl6 expressing cells in the context of antigen signaling and cognate T cell interactions in vivo. Furthermore, these results demonstrate that antigen encounter leads to the generation of distinct B cell states that can be discriminated on the basis of IRF4 and Bcl6 expression in vivo, which reflect mutual antagonism

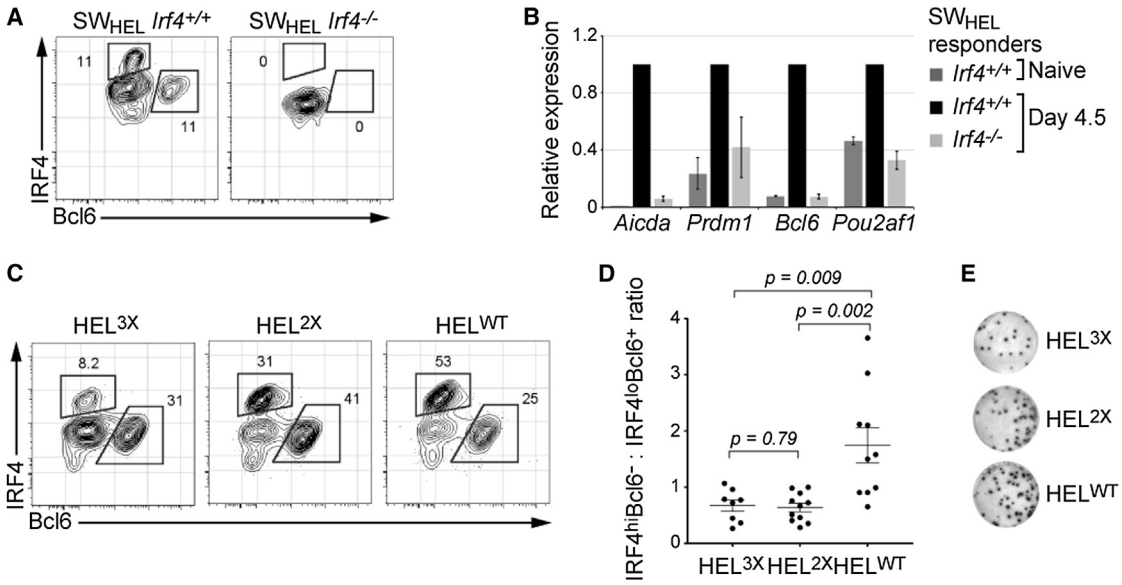

Figure 2. IRF4 Regulates GC B Cell Differentiation via the Activation of the *Bcl6* and *Pou2af1* Genes

Irf4$^{+/+}$ or *Irf4*$^{-/-}$ SW_{HEL} donor B cells were transplanted into CD45.1 hosts and immunized with HEL^{2X}SRBC.

(A) Four and a half days after immunization, donor-derived antigen specific cells were identified based on $B220^{+}CD45.2^{+}CD45.1^{-}$ phenotype and binding to HEL antigen. Expression of IRF4 and Bcl6 expression was then analyzed by intracellular staining.

(B) Cells described in (A) were sorted, and RNA was analyzed by qRT-PCR. Indicated transcripts were normalized to those from *Oct1* gene, and the data represents the average ± SEM of three independent experiments with two mice per group.

(C) WT SW_{HEL} donor B cells were adoptively transferred into CD45.1 hosts and immunized with indicated HEL variants conjugated to SRBC. Four and a half days after immunization, donor derived antigen specific cells were identified and analyzed as in (A).

(D) Quantitative analysis of experiments described in (C). The ratio of HEL-specific $IRF4^{hi}Bcl6^{-}$ to $IRF4^{lo}Bcl6^{+}$ expressing cells for individual mice is plotted from three independent experiments.

(E) ELISpot analysis of HEL-specific IgG secreting PC cells from experiments in (C); representative results are shown. See Figure S2 for quantitation.

between the GC B cell and plasma cell programs of gene expression.

We then tested whether IRF4 was required for transcriptional activation of the *Bcl6* and *Pou2af1* genes. SW_{HEL} responder cells were isolated 4.5 days following immunization (Figure S2D) and their transcripts analyzed by quantitative RT-PCR (qRT-PCR). Importantly expression of *Bcl6* and *Pou2af1* (encoding Obf1) were severely compromised in *Irf4*$^{-/-}$ SW_{HEL} B cells compared to their WT counterparts (Figure 2B). As expected, expression of the *Aicda* and *Prdm1* genes were also impaired (Klein et al., 2006; Sciammas et al., 2006). We note that Pax5 transcripts were comparable between *Irf4*$^{-/-}$ SW_{HEL} B cells and their WT counterparts (Figure S2E). Thus, the *Bcl6* and *Pou2af1* genes, which regulate GC B cell differentiation, are dependent on IRF4 for their induced expression in B cells upon antigen encounter in vivo.

Increased Antigen Affinity Favors Generation of $IRF4^{hi}$ Plasma Cells

Previously we have shown that increased antigen affinity augments BCR signaling-mediated expression of IRF4 and thus favors the generation of plasma cells at the expense of cells undergoing CSR in vitro (Sciammas et al., 2011). Given ability to analyze B cell dynamics in vivo on the basis of IRF4 and Bcl6 expression we tested whether varying antigen affinity in vivo had the predicted consequences on GC and plasma cell states. After adoptive transfer of SW_{HEL} cells, we immunized with a series of HEL variants that exhibit a 10,000 fold range in affinity for the HyHEL10 BCR (Paus et al., 2006). The highest-affinity antigen led to an increased proportion of $IRF4^{hi}Bcl6^{-}$ plasma cells (Figures 2C and 2D; Figure S2F). The enhancement in plasma cell generation was confirmed by HEL-specific ELISpot analysis (Figure 2E; Figure S2G). Thus, both in vitro as well as in vivo increasing the intensity of signaling through the BCR leads to greater expression of IRF4 and favors the generation of plasma cells.

Transient Expression of IRF4 Induces Generation of Bcl6 Expressing GC B Cells

To directly test consequences of manipulating IRF4 concentration on B cell-fate dynamics in vivo, we utilized a tet-inducible allele (Sciammas et al., 2011) with the SW_{HEL} transgenic system. This transgene is engineered to express IRF4 in a tet-responsive manner via the transcriptional activator (M2rtTA). The tet-inducible *Irf4* and SW_{HEL} transgenes were crossed onto the *Irf4*$^{-/-}$ background so that the former functioned as the sole source of IRF4 protein in vivo (Figure 3A). For the experiments using *Irf4*-inducible SW_{HEL} B cells, the CD45.1 host mice were crossed with the M2rtTA allele to prevent rejection of transplanted cells due to the neo-antigen effects of the bacterial transactivator protein. Following adoptive transfer of B cells into *CD45.1*$^{+}$*Rosa*$^{+/M2rtTA}$ congenic hosts and immunization with intermediate affinity HEL^{2X}, the mice were administered doxycycline (DOX) either continuously ("sustained") or just during the first two days after immunization ("pulsed"). Sustained

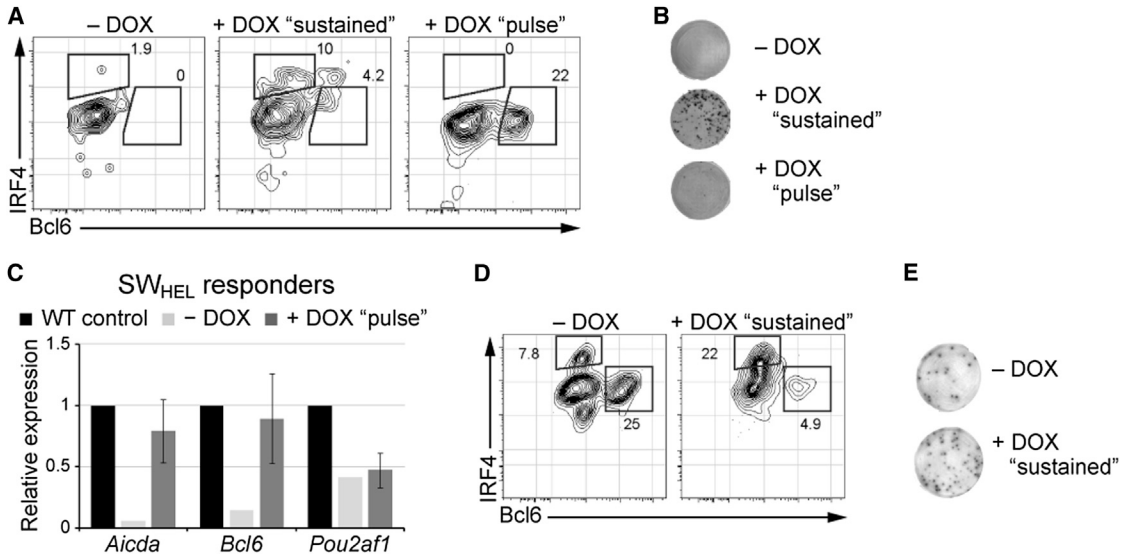

Figure 3. Inducible expression of *Irf4* regulates B cell-fate dynamics

(A) *Irf4*-inducible (*Irf4*$^{-/-}$) SW_{HEL} donor B cells transplanted into CD45.1*Rosa*$^{M2rtTA/+}$ hosts and immunized with HEL^{2X}SRBC. Mice were administered water lacking DOX (– DOX), containing DOX throughout the 5 day experiment (+ DOX "sustained") or containing DOX for the first 2 days only (+ DOX "pulse"). Five days after immunization, donor-derived antigen specific cells were identified and analyzed as in Figure 2A.

(B) Representative HEL-specific IgG ELISpot analysis from experiments in (A).

(C) Cells described in (A) were sorted and RNA was analyzed as in Figure 2B, the data represents the average ± SEM of three individual mice.

(D) *Irf4*-inducible (*Irf4*$^{+/+}$) HEL-specific SW_{HEL} donor B cells transplanted into CD45.1, *Rosa*$^{M2rtTA/+}$ hosts and immunized with HEL^{3X}SRBC. Mice were administered DOX as indicated in (A). Five days after immunization, donor-derived antigen-specific cells were identified and analyzed as in Figure 2A.

(E) Representative HEL-specific IgG ELISpot analysis from experiments in (D). Representative results from two independent experiments are shown; see Figure S3 for quantitation.

induction of the tet-inducible *Irf4* transgene led to the generation of IRF4^{hi}Bcl6^{-}- and Ig-secreting plasma cells (Figures 3A and 3B; Figure S3D). We note that rescued B cells secreted HEL-specific IgG demonstrating that sustained expression of IRF4 restored both CSR and secretory function (Figure 3B; Figure S3D). Importantly, transgenic expression of IRF4 also rescued the generation of Bcl6^{+} GC B cells (Figure 3A; Figure S3B and S3C). Strikingly, "pulsed" induction of IRF4 led only to the emergence of Bcl6 expressing GC B cells (Figure 3A; Figure S3B and S3C) that also expressed *Aicda* but not *Pou2af1* transcripts (Figure 3C). Importantly, plasma cells did not develop under these conditions (Figure 3A and 3B; Figure S3D). We note that the HEL-specific IgM spots observed with *Irf4*$^{-/-}$ cells most likely emanate from host-derived B cells because they are also seen in mice immunized with mock-conjugated SRBC (Figure S3D; data not shown). Thus, following antigen encounter, a transient burst of IRF4 expression appears sufficient to enable the generation of a stable population of GC B cells that express Bcl6 and AID.

Next, we tested whether increased expression of IRF4 in WT B cells might promote plasma cell differentiation at the expense of GC B cells. To do so, we adoptively transferred *Irf4*-inducible SW_{HEL} B cells on the *Irf4*$^{+/+}$ background into *CD45.1*$^{+}$*Rosa*$^{+/M2rtTA}$ congenic mice, immunized with HEL^{3X} and administered DOX in the drinking water (Figure S3E). Remarkably, SW_{HEL} responders in the "sustained" DOX group were impaired in their ability to generate Bcl6^{+} cells (Figure 3D; Figures S3B and S3C). DOX-mediated induction of the *Irf4* transgene led to an increase in IRF4^{hi} expressing cells and was accompanied by a corresponding increase in HEL-specific plasma cells (Figure 3E; Figure S3H). Interestingly, the increase in plasma cells was predominantly observed in the IgM class of HEL-specific cells (Figure S3H), as predicted by our model in which high IRF4 concentrations prevent durable AID expression. Thus transient induction of IRF4 is sufficient to induce the GC program. In contrast, sustained and higher concentrations of IRF4 terminate the GC program while promoting the generation of plasma cells.

Genomic Targeting Analysis of IRF4 and PU.1 in an Antigen-Dependent Differentiation System

To gain insight into IRF4 regulation of distinct programs of B cell gene expression, we performed ChIP-seq analyses in an antigen-specific in vitro system that results in CSR and efficient plasma cell differentiation (Figures S4A and S4B) (Sciammas et al., 2011). IRF4 expression is induced under these conditions with BCR engagement and exhibits a wide range of cellular concentrations at day 1 (Figure S4C). By day 3, a bimodal pattern of IRF4 expression is observable with cells expressing either low or high concentrations of IRF4, which correspond to those undergoing CSR or differentiating into plasma cells, respectively (Sciammas et al., 2006, 2011). We reasoned that kinetic analysis of the genome binding landscape of IRF4 in this cellular system might reveal a relationship between its differing concentrations and the regulation of distinct programs of gene expression. We note that these conditions do not promote the generation of GC B cells; however, given that AID is expressed and functions to promote SHM in these cells (Sciammas et al., 2011), we hypothesized that some molecular features of GC B cell

differentiation would be manifested in cells expressing the lower amounts of IRF4.

To analyze distinct modes of IRF4 genome targeting, we performed parallel ChIPseq analyses with its major interaction partner, PU.1 (Eisenbeis et al., 1995). This comparison enabled us to identify genomic regions that were targeted by IRF4 in conjunction with or in the absence of PU.1 (Figures S4A and S4D). Table S1 reports the details of sample processing with regard to sequencing, alignment and peak calls. The overall distribution of genomic sites of these two transcription factors is shown in Figure S4E and revealed that the majority of binding events were extragenic and occurred within 100 kbp of the nearest TSS. A small number of binding peaks were randomly chosen and validated by ChIP (Figure S4F).

To analyze the dynamics of IRF4 and PU.1 binding, we compiled coincident peaks between the day 1 and day 3 data sets (Figure S4D). Temporally-specific binding events were observed for both IRF4 and PU.1, suggesting that a shift in the genome binding landscape is associated with the bimodal expression of IRF4. Next, we determined the extent to which IRF4 targets the genome with or without PU.1 (Figures 4A and 4B). IRF4 cobound with PU.1 at a majority of the genomic sites. A third of IRF4 binding events were not associated with PU.1; this mode of IRF4 genome targeting is denoted IRF4 (not PU.1). Comparison of our data with DNaseI seq analysis in naive B cells (ENCODE data, Figure S4G) revealed ~90% of IRF4 (and PU.1) cotargeted regions (days 1 and 3) to be contained within DNaseI hypersensitive sites in naive B cells demonstrating that EICE motifs are located in accessible chromatin. In contrast, IRF4 (not PU.1) regions overlapped with $\leq$50% of the DNaseI sites present in naive B cells suggesting that this mode of IRF4 genomic targeting involved the de novo establishment of accessible regions.

Distinct DNA Motifs Comprise the IRF4 Cistrome

We searched for overrepresented sequence motifs by using the MEME pattern-finding algorithm in the IRF4 cistrome (Figures 4A and 4B). Within the IRF4 (and PU.1) bound regions, the EICE motif occurred with an incidence approaching 100%. This finding demonstrated the fundamental importance of the EICE motif in recruitment of IRF4 by PU.1 to genomic sites in differentiating B cells.

In contrast, within IRF4 (not PU.1)-bound regions, two distinct DNA motifs were enriched (Figure 4B). The first represented the ISRE, which is composed of two IRF motifs (GAAA) separated by two base pairs. The second motif was a canonical AP-1 motif that was often found near the peak's summit (Figure S4I). Inspection of the surrounding sequences identified an IRF motif (GAAA) either abutting or separated by four nucleotides from the AP-1 motif (Figure 4B; Figure S4H) suggesting the presence of an AP-1-IRF composite element (AICE) (Glasmacher et al., 2012). Accordingly, we found that BATF and IRF4 cobound to a sampling of these AICE motifs in B cells (Figure S4K). Thus, the IRF4 cistrome in B cells comprises three distinct DNA binding modes characterized by EICE, AICE, and ISRE motifs.

Within the IRF4 (not PU.1) peaks, the incidence of AICE and ISRE motifs was inverted between the day 1 and day 3 time points, and the ISRE predominated at day 3 (Figure 4B). This demonstrates that the nature of the IRF4 binding landscape shifts during the process of B cell differentiation, and the higher concentration of IRF4 is accompanied by increased occupancy of ISRE motifs.

IRF4 Binds the ISRE as a Dimer with Lower Affinity

Given the above finding, we analyzed the relative affinity of IRF4 for the ISRE and EICE motifs. An ISRE motif from *Prdm1* CNS9 (Sciammas et al., 2006) was used in electrophoretic mobility shift assays (EMSAs) (Figure 4C). IRF4 generated a protein-DNA complex (Figure 4C) that was competed by WT competitor DNA, but not ones in which one or both of the IRF sites were mutated. This suggested that IRF4 bound the ISRE as a dimer, which was confirmed by analyzing the migration of the protein-DNA complexes formed by mixing two different carboxy-terminal truncations of IRF4 (Figure S4J). Thus IRF4 binds the ISRE as a homodimer in contrast with its binding to an EICE as a heterodimer with PU.1 or to an AICE as a heterotrimer with a BATF-containing AP-1 complex.

To determine the relative affinity of IRF4-PU.1 heterodimeric or IRF4 homodimeric complexes for the EICE versus ISRE motifs, respectively, we analyzed binding over a wide range of IRF4 concentrations (Figures 4D and 4E). Whereas increasing IRF4 concentration in the presence of PU.1 resulted in saturation of IRF4 binding to the EICE, saturation was not observed for IRF4 binding (in the absence of PU.1) to the ISRE within the concentration range that was tested. These data demonstrated that IRF4 binds with higher affinity to EICE motifs as a heterodimer with PU.1 than to ISRE motifs as a homodimer and suggest that IRF4 is able to occupy EICE motifs at a lower concentration in vivo. Thus, higher IRF4 concentrations would be needed to drive binding onto ISRE motifs, and this is consistent with their increased utilization in differentiating IRF4^{hi} B cells at day 3 (Figure 4B; Figure S4C).

IRF4 Targeting of the *Prdm1* Locus

Our previous analysis had suggested that IRF4 directly activates *Prdm1* transcription to enable plasma cell differentiation. The ChIP-seq analysis confirmed that IRF4 bound to the CNS9 region in *Prdm1* (Figure 5A; Figure S5A). In addition, we identified multiple peaks surrounding the *Prdm1* gene that increased in intensity at day 3 (Figure S5A). Because IRF4 is necessary for promoting Blimp1 expression, we reasoned that IRF4 binding to the *Prdm1* locus may be required for the deposition of activating H3K4me1 and H3K27Ac chromatin marks. Analysis of WT B cells showed that these chromatin marks were present at low levels at some of these regions at the day 0 and day 1 time points but sharply increased at day 3 when *Prdm1* was maximally expressed (Figure S5B). In the absence of IRF4, these marks failed to accumulate not only at IRF4-targeted but also at nontargeted regions that included the *Prdm1* promoters (Figure S5C). Overall, this analysis demonstrates an extensive targeting landscape of IRF4 at the *Prdm1* locus that includes both IRF4 (and PU.1) and IRF4 (not PU.1) binding modes. Importantly IRF4 binding to multiple sites at the *Prdm1* locus appears to be required for the acquisition of an activated chromatin state.

IRF4 Targeting of *Bcl6* and *Pou2af1* Loci

Because *Bcl6* and *Pou2af1* expression is also dependent on IRF4, we sought to determine whether it targeted these genes.

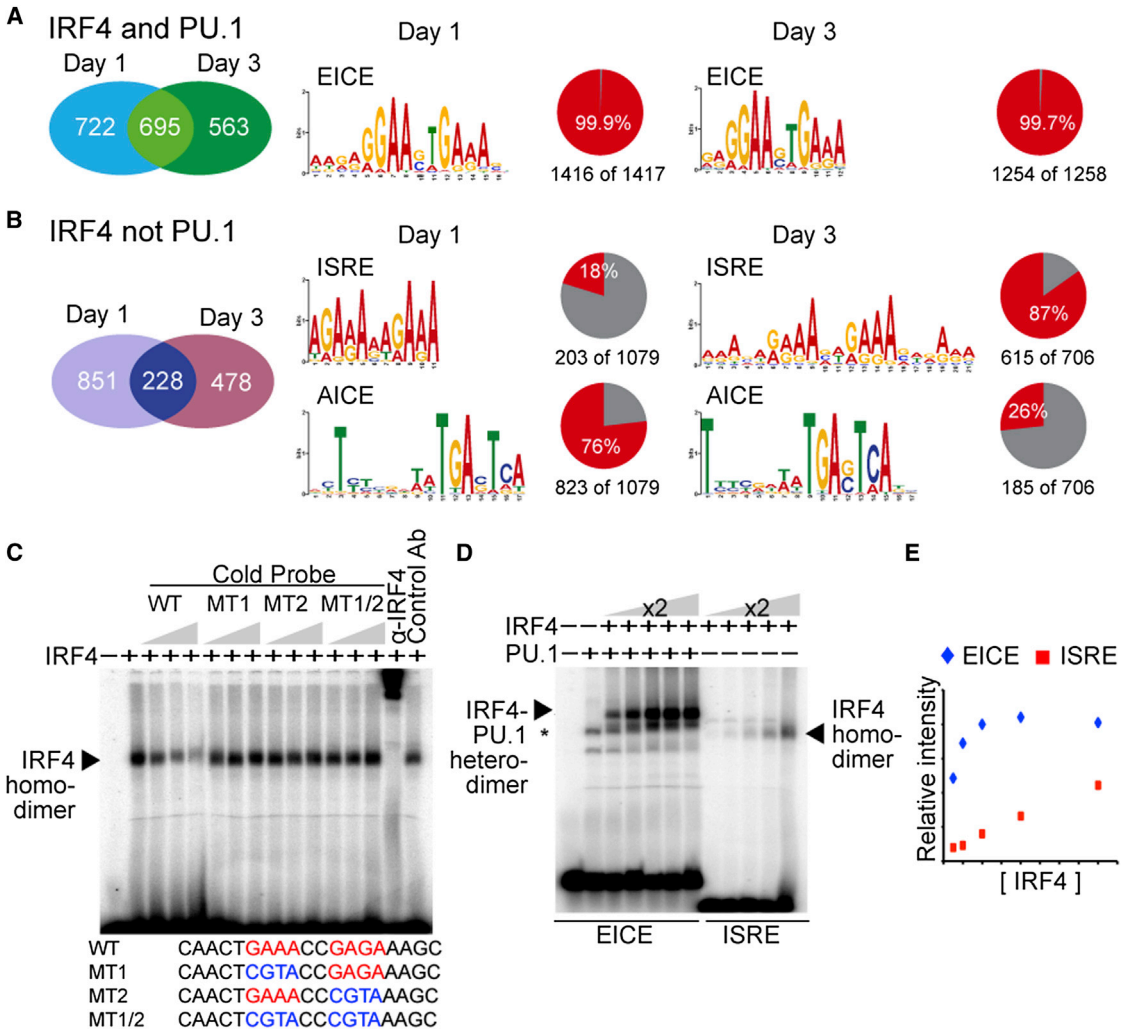

Figure 4. Analysis of IRF4 Cistrome in Antigen-Activated B Cells Reveals Three Distinct Motifs and Binding Modes

(A and B) B cells from B1-8i anti-NP knockin mice were stimulated with NP-Ficoll, CD40L, and interleukin-2 (IL-2), IL-4 and IL-5. On days 1 and 3, chromatin was crosslinked and processed for IRF4- and PU.1-specific ChIP coupled to massively parallel sequencing. Left panels display the union analysis of the number of IRF4 (and PU.1) or IRF4 (not PU.1) binding peaks, respectively, at day 1 or Day 3 after B cell stimulation. Right panels display overrepresented sequence motifs revealed by MEME in Logo format. The associated pie charts indicate the number of regions analyzed and the frequency with which the motif is found. EICE, ISRE, and AICE represent the Ets-IRF composite element, interferon sequence response element, and AP-1-IRF composite element, respectively.

(C) IRF4 binds with lower affinity to ISRE motifs than to EICE motifs. EMSA with the Blimp1 CNS9 ISRE sequence as probe. All binding reactions contained a WT probe and nuclear extract from IRF4-expressing 293T cells. Increasing amounts of competitor DNAs, WT, or mutant ISREs, were included as indicated. Anti-IRF4 or control antibodies were used in supershift assays to confirm identity of the IRF4 complex.

(D) Binding saturation curves of IRF4 to EICE or ISRE motifs. Binding reactions using the EICE DNA probe derived from the Ig Kappa 3′ enhancer were carried out in the presence of a constant amount of PU.1 protein. IRF4 protein was increased in 2-fold increments as indicated. The ISRE probe and binding reactions were conducted as in (C). Positions of relevant protein-DNA complexes are indicated by arrows.

(E) Densitometry analysis of (D). Data in (C) and (D) are representative of three independent experiments. See also Figure S4.

IRF4 bound to a region ~24 kbp upstream of the *Bcl6* gene (Figure 5B) and to several sites within the first intron. Notably, at the upstream position, PU.1 was found to cobind with IRF4 and this region coincided with a DNaseI hypersensitive site (Figure 5B; Figure S5D). We did not find evidence of IRF4 targeting the Bcl6 promoter as was shown in human B lymphoma cell lines (Saito et al., 2007). There were two prominent IRF4 (not PU.1) peaks within the first intron of *Pou2af1* gene (Figure 5C). IRF4 binding to sites in the *Bcl6* and *Pou2af1* genes diminished from day 1 to day 3 of B cell activation as compared with its occupancy of the *Prdm1* locus, which underwent an increase. To confirm targeting of the *Bcl6 and Pou2af1* genes by IRF4 in GC B cells, we performed ChIP analysis with such cells isolated from immunized mice. We observed binding of IRF4 to the aforementioned regions of the *Bcl6* and *Pou2af1* genes (Figure 5D). Thus these data, along with those in Figure 2B, demonstrate that IRF4 directly targets and activates the expression of key regulatory genes that are required for GC B cell differentiation.

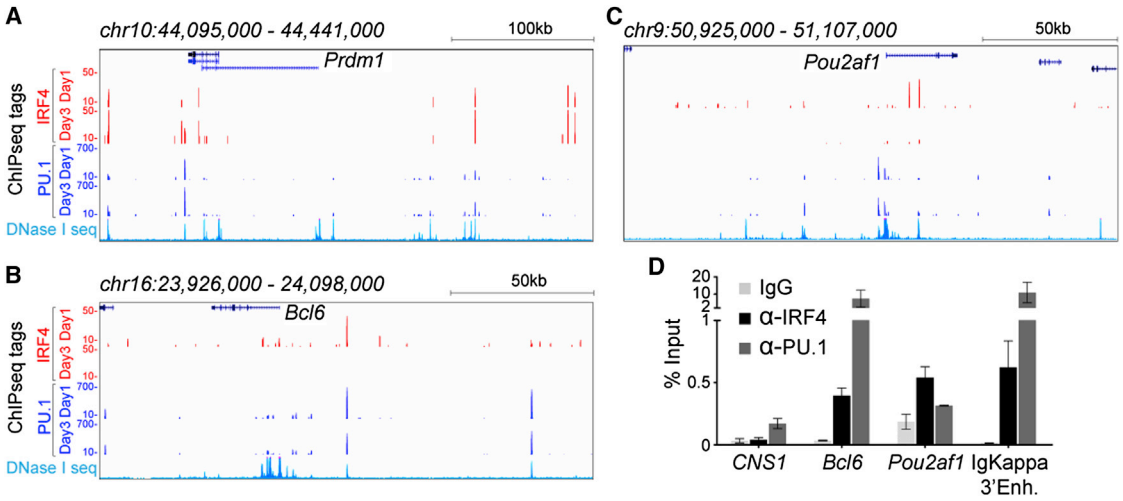

Figure 5. IRF4 Targets the *Prdm1*, *Bcl6*, and *Pou2af1* Genes

(A–C) ChIP-seq tag enrichment (y axis) is displayed as a histogram for the (A) *Prdm1* (Blimp1), (B) *Bcl6*, and (C) *Pou2af1* (Obf1) loci at indicated time points for antigen-activated B cells described in Figure 4. The x axis indicates the genomic interval (build mm9). The lowermost histogram in each panel shows genomic accessibility within naive CD19^{+} WT B cells, as assessed by DNaseI-seq (data downloaded from ENCODE).

(D) IRF4 binding to the *Bcl6* and *Pou2af1* loci in purified GC B cells. Enrichment values (% input chromatin) with control IgG, IRF4, and PU.1 antibodies are shown for indicated genomic regions: CNS1 (negative control), *Bcl6*, *Pou2af1*, and *Igkappa* 3′ enhancer (positive control). The average enrichment and SEM is from two independent experiments. See also Figure S5.

Divergent IRF4 Binding Modes Correlate with Complementary Patterns of Gene Activity

We next analyzed how the distinct modes of IRF4 targeting correlate with IRF4 dependent gene expression programs that are reflective of the "GC-like" and plasma cell states. Thus we performed genome-wide transcriptome analyses and compared WT or *Irf4*-inducible B cells (Sciammas et al., 2011) on the *Irf4*$^{-/-}$ background.

We reasoned that we could relate distinct patterns of gene expression to divergent modes of IRF4 genome targeting by analyzing the expression changes between cellular conditions in which IRF4 is expressed to varying extents at the different time points. To this end, we employed Expectation Maximization of Binding and Expression Profiles (EMBER) (Maienschein-Cline et al., 2011), which uses an unsupervised machine learning algorithm to infer target genes from transcription factor binding and expression data. EMBER scores genes that are likely regulated by a given transcription factor within 100 kpb of its binding peaks based on their conforming to an overrepresented gene expression pattern (see Supplemental Information for further details).

We applied EMBER to the IRF4 (and PU.1) and IRF4 (not PU.1) peaks at the day 1 and day 3 time points (Figures 4A and 4B). The EMBER analysis is shown in Figure 6A and Table S2. The numbers in the upper left hand boxes of each graph indicate the number of peaks that were assigned at least one target gene (Figure 6A). Roughly half of all genome targeting events (compare to the number of peaks in Figures 4A and 4B) scored above a statistical threshold (see Supplemental Information). To simplify analysis of the gene expression data, we binned differential expression between pairwise sample comparisons into five categories: (++) large upregulation, (+) small upregulation, (0) no change, (–) small downregulation, and (– –) large downregulation (see Supplemental Information). Each of the pairwise gene expression comparisons are plotted against the log-likelihood ratio of finding a given differential expression pattern. IRF4 peak-associated trends in differential gene expression are represented as changes in the relative sizes of colored bars corresponding to each of the five bins of differential expression. For example, in Figure 6A, in the IRF4 (and PU.1) day 1 expression pattern (top left), the large bright green bars in the fourth, fifth, and sixth columns indicate that the majority of inferred target genes tend to be strongly downregulated in the presence of IRF4 (either in WT cells or in *Irf4*$^{-/-}$ cells after restoration of IRF4 expression with DOX). Conversely, the much smaller red bars in the same columns indicate that very few of the inferred gene targets are strongly upregulated in the presence of IRF4.

EMBER analysis revealed three dominant patterns of transcriptional control by IRF4 (and PU.1) binding versus IRF4 (not PU.1) binding events (Figure 6A). In the first pattern, inferred target genes associated with IRF4 (and PU.1) binding tended to be repressed regardless of time point (the green bars corresponding to mild and strong repression are large). This unexpected finding is consistent with an IRF4-dependent manner of regulation because (1) these genes were derepressed in the absence of IRF4 and (2) the same genes were repressed when IRF4 expression was restored by DOX-mediated induction of the inducible allele of *Irf4* in *Irf4*$^{-/-}$ B cells (Figure 6A). In the second pattern, genes associated with IRF4 (not PU.1) binding were preferentially activated at day 1. The third pattern comprises a mixture of up- and downregulated targets of IRF4 (not PU.1) on day 3. We note that the transition in the nature of transcriptional output accompanies both the change in IRF4 concentration (Figure S4C) as well as the differentiation state of these cells (Figure S4B). Collectively, this analysis shows that IRF4 (not PU.1) genome targeting, regardless of time, is associated with markedly different behaviors of gene expression compared to

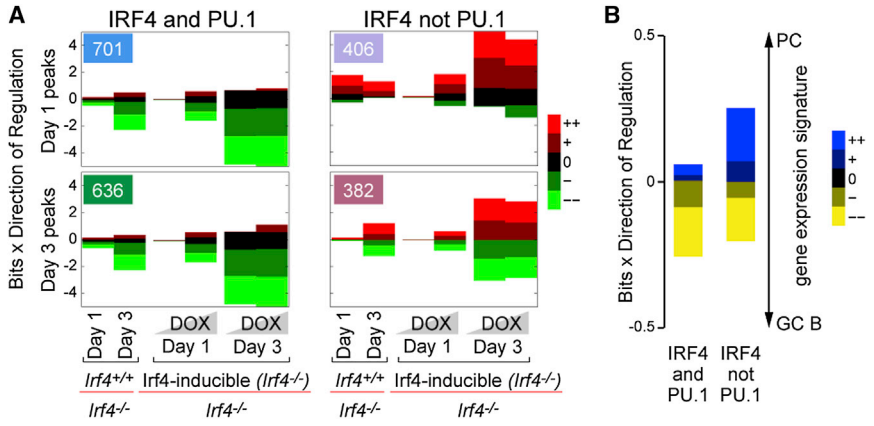

Figure 6. IRF4 (and PU.1) and IRF4 (not PU.1) Genome Targeting Are Associated with Distinct Patterns of Transcriptional Regulation

(A) Genome-wide expression data was derived from purified B cells isolated from WT ($Irf4^{+/+}$), mutant ($Irf4^{-/-}$), or *Irf4*-inducible mice that were stimulated with CD40L and cytokines. Total RNA was isolated on days 1 and 3 and processed for Affymetrix arrays. B cells from the *Irf4*-inducible mice were also cultured in the presence of 16 ng/mL or 100 ng/mL doxycycline (DOX) to induce the expression of the *Irf4* transgene, indicated by the shaded gradients on the x axis. EMBER expression patterns for the four peak combinations (IRF4 at days 1 and 3 with and without PU.1). The numbers in the upper lefthand boxes of each graph indicate the number of peaks that scored above a threshold and were assigned at least one target gene. The x axis displays pairwise comparisons between expression measurements (specifically WT cells versus $Irf4^{-/-}$ cells or *Irf4*-inducible cells (on the $Irf4^{-/-}$ background) with and without DOX). The size of each bar in the y axis indicates the significance of changes in expression and the color indicates the nature of the change; see (Maienschein-Cline et al., 2011) for further details.

(B) Day 3 inferred target gene expression in the context of ex vivo antigen specific GC B cell and plasma cell transcriptomes (from NCBI GEO). Data presented as in (A). See also Figure S6.

those associated with IRF4 (and PU.1) genome targeting, suggesting that each binding mode functions to control distinct developmental programs.

Divergent IRF4 Binding Modes Correlate with Distinct Developmental Programs

To substantiate the hypothesis that IRF4 (and PU.1) and IRF4 (not PU.1) modes of genome targeting regulate different developmental programs, we tested whether the expression patterns of inferred target genes obtained from differentiated cells at the day 3 time point correlated with plasma cell or GC B cell states. To perform this analysis, we used transcriptome experiments derived from ex vivo sorted antigen-specific plasma cells and GC B cells (Luckey et al., 2006). By using these data from GEO, we compared GC B cell and plasma cell transcriptomes and classified differential gene expression by using the same discrete binning scheme as above (++, +, 0, –, – –). Then, by using inferred target genes from either IRF4 (and PU.1) or IRF4 (not PU.1) day 3 peaks, we computed the log odds ratio of finding preferential expression of these genes in plasma cells or GC B cells (Figure 6B; Figure S6A; Table S2). With some exceptions, we found that the majority of IRF4 (and PU.1) inferred target genes were expressed at lower levels in plasma cells compared to GC B cells (large yellow bar). In contrast, inferred target genes associated with IRF4 (not PU.1) binding at day 3 enriched for a substantial set of genes that were expressed at higher levels in plasma cells compared to GC B cells (large bright blue bar). Similar trends were observed when we analyzed the naive to GC B cell and the naive to plasma cell transitions (Figures S6B and S6C). These data indicate that, during the transition of a naive or GC B cell to a plasma cell, both IRF4 (and PU.1) and IRF4 (not PU.1) binding events are associated with the repression of GC genes. In contrast, IRF4 (not PU.1) binding, particularly to the ISRE motif seems to preferentially function in activation of the PC program of gene expression. The proposed functions of these distinct modes of IRF4 genome targeting in relation to its intracellular concentrations and B cell fate dynamics are depicted in Figure S7.

To further corroborate the finding that each binding mode is controlling distinct developmental programs, we determined whether the inferred target genes controlled by IRF4 (and PU.1) and IRF4 (not PU.1) genome targeting were associated with different functional classes of genes. Whereas genes associated with IRF4 (and PU.1) binding enriched for immune and inflammatory response categories, the IRF4 (not PU.1)-associated genes enriched for cell biological categories including endoplasmic reticulum functions (Figure S6D; Table S3). Many of these latter genes are important for the differentiation of specialized secretory cells suggesting that the IRF4 (not PU.1) targeting mode involving ISREs specifies the functional state of plasma cells.

DISCUSSION

We have demonstrated an essential and cell-intrinsic role for IRF4 in generating GC B cells. IRF4 does so in part by activating expression of the *Bcl6* and *Pou2af1* genes. Our combined genetic analyses involving conditional deletion of the *Irf4* gene prior to B cell activation as well as its transient expression by using the *Irf4*-inducible allele define the temporal requirement for IRF4 in promoting GC B cell fate to the first few days after antigen encounter. The results strongly suggest that IRF4 is required for initiation, but not maintenance of the GC state, and the latter is dependent on sustained expression of Bcl6. It follows that IRF4 is required for the activation but not maintenance of expression of the *Bcl6 gene.* In contrast, expression of the *Pou2af1* gene appears to continuously depend upon IRF4. Intriguingly, the latter gene along with IRF4 also functions in regulating plasma cell differentiation (Corcoran et al., 2005). Given that high and sustained expression of IRF4 antagonizes the GC state, these findings account for transient action of IRF4 in generating

GC B cells and its downregulation in such cells. It will be interesting to determine whether in GC B cells negative feedback by Bcl6 serves to directly repress the *Irf4* gene, as has been observed in cell lines (Alinikula et al., 2011).

Our key conclusion that IRF4 functions in a cell-intrinsic manner to regulate GC B cell differentiation differs from that reached by a recent report (Bollig et al., 2012). We note that our findings are based on the use of three distinct alleles of *Irf4*: germline, conditional, and tet-inducible. Importantly, the *Irf4*-conditional allele ($Irf4^{fl/fl}$) displays a GC B cell defect when CRE expression is driven by the CD19 locus but not by the Cγ1 locus. Finally, the tet-inducible *Irf4* allele allowed us to unambiguously demonstrate that Bcl6 and AID expression can be induced in $Irf4^{-/-}$ B cells in an IRF4-dependent manner. Bollig et al. demonstrate a role for IRF4 in T follicular helper cell differentiation. We therefore propose that IRF4 may direct T follicular helper cell differentiation by directly activating Bcl6 expression, as is the case in B cells.

By using genome-wide analysis in a model system involving antigen-dependent B cell differentiation, three distinct modes of IRF4 binding to its target sequences have been delineated. The dominant mode (representing two thirds of the total) involves cobinding of IRF4 with PU.1 to EICE motifs. Two additional modes, both of which are PU.1 independent, involve IRF4 binding to either an ISRE or AICE motif. Co-occupancy of the EICE motif by PU.1 and IRF4 is associated with regulation of genes involved in B cell activation and function. Molecular redundancy between PU.1 and SpiB in the Ets family, as well as between IRF4 and IRF8 in the IRF family, can result in the targeting of the EICE motif by four distinct Ets-IRF ternary complexes (Eisenbeis et al., 1995). Accordingly, these complexes can play either redundant or unique roles in B cell development, activation, and terminal differentiation. Importantly, although IRF4 and IRF8 function redundantly in the differentiation of pre-B cells (Lu et al., 2003), IRF4 is uniquely required for the GC response and plasma cell differentiation (Feng et al., 2011; Klein et al., 2006; Sciammas et al., 2006). Given that SpiB is uniquely important for the differentiation of GC B cells along with the observation that IRF8 is expressed at high levels in GC B cells, it will be interesting to determine whether occupancy of the EICE motif in this cellular context shifts to these factors.

A second mode of IRF4 binding is observed on composite AP-1-IRF motifs (AICE). This unusual motif has been observed by us in the context of T cells, where it functions as the dominant mode of IRF4 genomic targeting, given that these cells do not express PU.1 or SpiB (Glasmacher et al., 2012). We have demonstrated that this composite motif directs cooperative binding of IRF4 with BATF heterodimers belonging to the AP-1 family. As $Batf^{-/-}$ B cells partially phenocopy $Irf4^{-/-}$ B cells (Betz et al., 2010; Ise et al., 2011), it will be informative to analyze the molecular consequences of IRF4-BATF family complexes that assemble on AICE motif-containing genes. In accord with a signal-dependent mode of gene regulation by AP-1 family members, the AICE motif is observed at high incidence in DNA bound regions at the day 1 time point, soon after BCR signaling initiated by antigen encounter. At this time point, B cells are forming blasts and initiating the gene regulatory programs necessary for subsequent differentiation. The integration of IRF4 with the AP-1 system at this stage, both of which are controlled by BCR signaling, suggests that they could be important for effecting the downstream transcriptional responses that are triggered by differential BCR signaling; i.e., low- or high-affinity antigen or levels of coreceptor engagement.

The third mode of IRF4 binding in the B cell genome involves classical ISREs. We demonstrate that IRF4 binds the ISRE as a homodimer, and this interaction is of lower affinity than the PU.1-IRF4 interaction with the EICE motif. Accordingly, binding to the ISRE is preferentially observed at the day 3 time point of B cell differentiation when IRF4 protein levels peak. The day 3 time point represents a stage where a majority of the B cells in the culture system have undergone differentiation into plasma cells. Intriguingly, the increased usage of the ISRE in plasma cells suggests an association of this regulatory element with structural genes important for their differentiation. Indeed, such target genes are enriched for those that encode secretory functions. Although the concept of differing concentrations of a transcription factor regulating distinct cell fates has been suggested to be widely operative in mammalian cell differentiation (see De-Koter and Singh, 2000), its molecular basis has proven difficult to elucidate. Our results provide an appealing molecular explanation for the requirement of higher concentrations of IRF4 in regulating plasma cell differentiation by enabling occupancy of low affinity ISRE motifs that are associated with plasma cell genes.

Based on experimental and mathematical analyses, we have proposed a mechanism of kinetic control in which the initial rate of IRF4 accumulation, driven by the strength of BCR signaling, controls a gene regulatory network that orchestrates cell fate decisions between cells undergoing CSR, a ''GC-like'' state, versus cells differentiating into plasma cells (Sciammas et al., 2011). In this model, low affinity or avidity antigen interactions with the BCR favor a longer duration of a ''GC-like'' state before plasma cell differentiation. In contrast, high affinity or avidity antigen interactions with the BCR limit the period of time in which AID is expressed and therefore promote plasma cell generation accompanied with relatively low levels of CSR and SHM. Herein, we corroborate and extend this regulatory model. Specifically, as evidenced by the ''pulsed'' experiment, we propose that transient expression of IRF4 in GC B cells ($IRF4^{lo}Bcl6^{+}$) serves to ''reset'' the mechanism of kinetic control initiated by the first exposure to antigen. Hence, kinetic control would be reinstated during positive selection of somatically hypermutated GC B cells upon their interaction with antigen displayed by follicular dendritic cells. Specifically, those clones accumulating mutations that confer higher affinity to their BCR would induce increased levels of IRF4 expression, both as a function of BCR signaling and CD40 signaling by T helper cells, and thus differentiate into plasma cells. In support of this notion, it has been found that post-GC plasma cells are preferentially enriched for high affinity SHM-dependent mutations (Phan et al., 2006; Smith et al., 1997). In contrast, those clonotypes exhibiting lower affinity conferring mutations would induce lower levels of IRF4 expression and differentiate into memory B cells or undergo new rounds of SHM and selection (Smith et al., 1997; Victora et al., 2010). Given that GC B cells express high amounts of Bcl6, it will be interesting to determine whether selection into the high affinity cell pool involves a steeper magnitude of IRF4 induction to overcome repression by Bcl6.

EXPERIMENTAL PROCEDURES

Mice

The generation of the *Irf4*$^{-/-}$ and *Irf4*-inducible mice has been previously described (Mittrücker et al., 1997; Sciammas et al., 2011). The B1-8i gene targeted mice were a generous gift of K. Rajewsky. SW_{HEL} mice have been previously described (Phan et al., 2005) and were used to cross to *Irf4*$^{-/-}$ mice and *Irf4*-inducible mice. Conditional *Irf4*$^{fl/fl}$ mice (Klein et al., 2006) were crossed to *CD19*$^{+/CRE}$ mice. Mice were housed in specific pathogen-free conditions and were used and maintained in accordance of the Institutional Animal Care and Use Committee guidelines.

ChIP and ChIP-Seq

ChIP was performed by using anti-IRF4, -PU.1, -H3K4me1, -H3K27Ac, and control IgG antibodies (Santa Cruz Biotech. and Abcam) (Sciammas et al., 2006). For massively parallel sequencing, 200 μg of chromatin fragments were immunoprecipitated by using anti-IRF-4 and anti-PU.1 antibodies, and DNA libraries were prepared. DNA was sequenced by using the Illumina GA2, data was processed with the Solexa pipeline package, and sequences were aligned to the mouse genome (mm9) by using ELAND software. Further details are available in the Supplemental Information.

Generation of Mixed Bone Marrow Chimeric Mice and SRBC Immunization

Bone marrow was collected from the long leg bones of WT CD45.1/2 heterozygous mice and from *Irf4*$^{+/+}$ or *Irf4*$^{-/-}$ (both CD45.2) mice and mixed together in equal numbers. Cells were injected into irradiated (2 × 550 rads) WT CD45.1 mice. Eight weeks after adoptive transfer, mice were immunized with sheep RBC (Lampire Biologicals) intraperitoneally, and the GC response was quantified by flow cytometry 7 days later. Conditional *Irf4*$^{fl/fl}$ mice were bred to CD19C$^{+/CRE}$, immunized with SRBC, and spleens were analyzed 14 days later. Further details are available in the Supplemental Information.

Adoptive Transfer of SW_{HEL} B Cells

SW_{HEL} mice were crossed to *Irf4*-inducible or *Irf4*$^{-/-}$ mice and used for adoptive transfer experiments using established methods (Phan et al., 2005). Doxycline (DOX, Sigma) was administered in drinking water that contained 1% (w/v) sucrose, at a concentration of 0.5 mg/mL; the control group was fed sucrose water only and the "pulse" group was changed to sucrose water only after the initial DOX treatment. Further details regarding CFSE labeling, numbers of transferred cells, SRBC-conjugated antigens, and sorting are available in the Supplemental Information.

Flow Cytometry and ELISpot Assays

RBC-depleted spleen cell suspensions were prepared, stained, and analyzed on the LSR II flow cytometer, and the resulting data was processed by using FlowJo software (Tree Star, Inc.). HEL+ cells were identified as described (Phan et al., 2005). Detection of Bcl6 was performed by fixing and permeabilizing cells with Fix/Perm staining kit (eBioscience) and staining with anti-Bcl6 (BD). Detection of IRF4 was performed as previously described (Sciammas et al., 2011). For ELISpot analysis, total splenocytes were cultured for 6 hr on plates coated with HEL (Sigma) and processed with anti-IgM and anti-IgG antibodies as previously described (Sciammas et al., 2006). Further details are available in the Supplemental Information.

RNA Preparation, Microarray, and RT-PCR Analysis

For transcriptome analysis, total RNA was prepared from triplicate cell samples by using Trizol and processed for hybridization to Affymetrix mouse 430A chips by using standard procedures. For qRT-PCR analysis of sorted SW_{HEL} B cells, total RNA was prepared by sorting 5,000 cells directly into RLT buffer from the RNeasy Micro Kit (QIAGEN). Further details are available in the Supplemental Information.

ACCESSION NUMBERS

The SuperSeries, GSE46608, which includes expression (GSE46606) and ChIP-seq (GSE46607) data have been deposited in the GEO database.

SUPPLEMENTAL INFORMATION

Supplemental Information includes seven figures, four tables, and Supplemental Experimental Procedures and can be found with this article online at http://dx.doi.org/10.1016/j.immuni.2013.04.009.

ACKNOWLEDGMENTS

We thank Q. Wang and J. Harakh for animal husbandry and injections. We thank the UC Flow Cytometry Core Facility and the Bendelac laboratory for assistance with cell sorting and analysis, respectively. We are grateful to K. Michelini and J. Zekos for operating the Illumina Genome Analyzer II at the University of Chicago (supported by the Howard Hughes Medical Institute). Research was supported by the US Department of Energy (DOE) Computational Science Graduate Fellowship Program (M.M.-C.), CLL Global Research Foundation (U.K.), the National Institutes of Health (P50, GM081892 to A.R.D. and H.S.), the National Kidney Foundation, IL Division and the Illinois Department of Public Health, Juvenile Diabetes and Islet Transplantation Research Grant (R.S.).

Received: April 25, 2012
Accepted: February 4, 2013
Published: May 16, 2013

REFERENCES

Alinikula, J., Nera, K.P., Junttila, S., and Lassila, O. (2011). Alternate pathways for Bcl6-mediated regulation of B cell to plasma cell differentiation. Eur. J. Immunol. *41*, 2404–2413.

Allman, D., Lindsley, R.C., DeMuth, W., Rudd, K., Shinton, S.A., and Hardy, R.R. (2001). Resolution of three nonproliferative immature splenic B cell subsets reveals multiple selection points during peripheral B cell maturation. J. Immunol. *167*, 6834–6840.

Betz, B.C., Jordan-Williams, K.L., Wang, C., Kang, S.G., Liao, J., Logan, M.R., Kim, C.H., and Taparowsky, E.J. (2010). Batf coordinates multiple aspects of B and T cell function required for normal antibody responses. J. Exp. Med. *207*, 933–942.

Bollig, N., Brüstle, A., Kellner, K., Ackermann, W., Abass, E., Raifer, H., Camara, B., Brendel, C., Giel, G., Bothur, E., et al. (2012). Transcription factor IRF4 determines germinal center formation through follicular T-helper cell differentiation. Proc. Natl. Acad. Sci. USA *109*, 8664–8669.

Brass, A.L., Zhu, A.Q., and Singh, H. (1999). Assembly requirements of PU.1-Pip (IRF-4) activator complexes: inhibiting function in vivo using fused dimers. EMBO J. *18*, 977–991.

Corcoran, L.M., Hasbold, J., Dietrich, W., Hawkins, E., Kallies, A., Nutt, S.L., Tarlinton, D.M., Matthias, P., and Hodgkin, P.D. (2005). Differential requirement for OBF-1 during antibody-secreting cell differentiation. J. Exp. Med. *201*, 1385–1396.

DeKoter, R.P., and Singh, H. (2000). Regulation of B lymphocyte and macrophage development by graded expression of PU.1. Science *288*, 1439–1441.

Eisenbeis, C.F., Singh, H., and Storb, U. (1995). Pip, a novel IRF family member, is a lymphoid-specific, PU.1-dependent transcriptional activator. Genes Dev. *9*, 1377–1387.

Feng, J., Wang, H., Shin, D.M., Masiuk, M., Qi, C.F., and Morse, H.C., 3rd. (2011). IFN regulatory factor 8 restricts the size of the marginal zone and follicular B cell pools. J. Immunol. *186*, 1458–1466.

Garrett-Sinha, L.A., Dahl, R., Rao, S., Barton, K.P., and Simon, M.C. (2001). PU.1 exhibits partial functional redundancy with Spi-B, but not with Ets-1 or Elf-1. Blood *97*, 2908–2912.

Glasmacher, E., Agrawal, S., Chang, A.B., Murphy, T.L., Zeng, W., Vander Lugt, B., Khan, A.A., Ciofani, M., Spooner, C., Rutz, S., et al. (2012). A Genomic Regulatory Element That Directs Assembly and Function of Immune-Specific AP-1-IRF Complexes. Science *338*, 975–980.

Goodnow, C.C., Vinuesa, C.G., Randall, K.L., Mackay, F., and Brink, R. (2010). Control systems and decision making for antibody production. Nat. Immunol. *11*, 681–688.

Ise, W., Kohyama, M., Schraml, B.U., Zhang, T., Schwer, B., Basu, U., Alt, F.W., Tang, J., Oltz, E.M., Murphy, T.L., and Murphy, K.M. (2011). The transcription factor BATF controls the global regulators of class-switch recombination in both B cells and T cells. Nat. Immunol. *12*, 536–543.

Klein, U., Casola, S., Cattoretti, G., Shen, Q., Lia, M., Mo, T., Ludwig, T., Rajewsky, K., and Dalla-Favera, R. (2006). Transcription factor IRF4 controls plasma cell differentiation and class-switch recombination. Nat. Immunol. *7*, 773–782.

Lu, R., Medina, K.L., Lancki, D.W., and Singh, H. (2003). IRF-4,8 orchestrate the pre-B-to-B transition in lymphocyte development. Genes Dev. *17*, 1703–1708.

Luckey, C.J., Bhattacharya, D., Goldrath, A.W., Weissman, I.L., Benoist, C., and Mathis, D. (2006). Memory T and memory B cells share a transcriptional program of self-renewal with long-term hematopoietic stem cells. Proc. Natl. Acad. Sci. USA *103*, 3304–3309.

Maienschein-Cline, M., Zhou, J., White, K.P., Sciammas, R., and Dinner, A.R. (2011). Discovering Transcription Factor Regulatory Targets Using Gene Expression and Binding Data. Bioinformatics *28*, 206–213.

Mittrücker, H.W., Matsuyama, T., Grossman, A., Kündig, T.M., Potter, J., Shahinian, A., Wakeham, A., Patterson, B., Ohashi, P.S., and Mak, T.W. (1997). Requirement for the transcription factor LSIRF/IRF4 for mature B and T lymphocyte function. Science *275*, 540–543.

Muto, A., Ochiai, K., Kimura, Y., Itoh-Nakadai, A., Calame, K.L., Ikebe, D., Tashiro, S., and Igarashi, K. (2010). Bach2 represses plasma cell gene regulatory network in B cells to promote antibody class switch. EMBO J. *29*, 4048–4061.

Nutt, S.L., Taubenheim, N., Hasbold, J., Corcoran, L.M., and Hodgkin, P.D. (2011). The genetic network controlling plasma cell differentiation. Semin. Immunol. *23*, 341–349.

Paus, D., Phan, T.G., Chan, T.D., Gardam, S., Basten, A., and Brink, R. (2006). Antigen recognition strength regulates the choice between extrafollicular plasma cell and germinal center B cell differentiation. J. Exp. Med. *203*, 1081–1091.

Phan, T.G., Gardam, S., Basten, A., and Brink, R. (2005). Altered migration, recruitment, and somatic hypermutation in the early response of marginal zone B cells to T cell-dependent antigen. J. Immunol. *174*, 4567–4578.

Phan, T.G., Paus, D., Chan, T.D., Turner, M.L., Nutt, S.L., Basten, A., and Brink, R. (2006). High affinity germinal center B cells are actively selected into the plasma cell compartment. J. Exp. Med. *203*, 2419–2424.

Saito, M., Gao, J., Basso, K., Kitagawa, Y., Smith, P.M., Bhagat, G., Pernis, A., Pasqualucci, L., and Dalla-Favera, R. (2007). A signaling pathway mediating downregulation of BCL6 in germinal center B cells is blocked by BCL6 gene alterations in B cell lymphoma. Cancer Cell *12*, 280–292.

Sciammas, R., Shaffer, A.L., Schatz, J.H., Zhao, H., Staudt, L.M., and Singh, H. (2006). Graded expression of interferon regulatory factor-4 coordinates isotype switching with plasma cell differentiation. Immunity *25*, 225–236.

Sciammas, R., Li, Y., Warmflash, A., Song, Y., Dinner, A.R., and Singh, H. (2011). An incoherent regulatory network architecture that orchestrates B cell diversification in response to antigen signaling. Mol. Syst. Biol. *7*, 495.

Smith, K.G., Light, A., Nossal, G.J., and Tarlinton, D.M. (1997). The extent of affinity maturation differs between the memory and antibody-forming cell compartments in the primary immune response. EMBO J. *16*, 2996–3006.

Su, G.H., Chen, H.M., Muthusamy, N., Garrett-Sinha, L.A., Baunoch, D., Tenen, D.G., and Simon, M.C. (1997). Defective B cell receptor-mediated responses in mice lacking the Ets protein, Spi-B. EMBO J. *16*, 7118–7129.

Victora, G.D., Schwickert, T.A., Fooksman, D.R., Kamphorst, A.O., Meyer-Hermann, M., Dustin, M.L., and Nussenzweig, M.C. (2010). Germinal center dynamics revealed by multiphoton microscopy with a photoactivatable fluorescent reporter. Cell *143*, 592–605.